Tripartite interactions between two phase qubits and a resonant cavity

F. Altomare[1*], J. I. Park[1*], K. Cicak[1], M. A. Sillanpää[1]†, M. S. Allman[1,3], D. Li[1], A. Sirois[1,3], J. A. Strong[1,3], J. D. Whittaker[1,3], and R. W. Simmonds[1]

[1]*National Institute of Standards and Technology, 325 Broadway, Boulder CO 80305, USA*

†*Present address: Helsinki University of Technology, Espoo P.O. Box 2200 FIN-02015 HUT, Finland*

[3]*University of Colorado, 2000 Colorado Ave, Boulder, CO 80309-0390, USA*

**These authors contributed equally to this work.*

The creation and manipulation of multipartite entangled states is important for advancements in quantum computation[1] and communication[2–4], and for testing our fundamental understanding of quantum mechanics[5] and precision measurements[6]. Multipartite entanglement has been achieved by use of various forms of quantum bits (qubits), such as trapped ions[7,8], photons[9], and atoms passing through microwave cavities[10]. Quantum systems based on superconducting circuits have been used to control pair-wise interactions of qubits, either directly[11–13], through a quantum bus[14,15], or via controllable coupling[16]. Here, we describe the first demonstration of coherent interactions of three directly coupled superconducting quantum systems, two phase qubits and a resonant cavity. We introduce a simple Bloch-sphere-like representation to help one visualize the unitary evolution of this tripartite system as it shares a single microwave photon. With careful control and timing of the initial conditions, this leads to a protocol for creating a rich variety of entangled states. Experimentally,

we provide evidence for the deterministic evolution from a simple product state, through a tripartite W-state, into a bipartite Bell-state. These experiments are another step towards deterministically generating multipartite entanglement in superconducting systems with more than two qubits.

With the development of quantum information science[1], entanglement of multi-particle systems has become a resource for a new information technology. In particular, three-particle or tripartite entanglement allows for teleportation[2], secret sharing[4], and dense coding[17], with connections to cosmology[18]. Over the last decade, the development of exquisite control over quantum systems has led to various demonstrations of tripartite entanglement[8–10]. Genuine tripartite entanglement is delineated by two inequivalent classes of states[19]: GHZ (Greenberger-Horne-Zeilinger) and W, where the W-state involves only a single photon shared amongst three systems. Utilizing multipartite entanglement in a solid-state-qubit system has only recently received theoretical attention[20–22]. Thus far in superconducting systems, bipartite entanglement has been verified by two-qubit quantum state tomography[13] and used to perform a quantum algorithm[15]. Spectroscopic evidence for three-particle entanglement was observed for two current-biased phase qubits coupled to a lumped element LC-cavity as well as for Transmon qubits.[23,24] In the experiments described below, we first verify the spectroscopic signature of three coupled systems. Next, we demonstrate coherent interactions. Frequency detuning of the third system is used to verify the proper change in the time evolution of two versus three coupled systems. Finally, we describe a free-evolution process and a visualization technique as a method for deterministically preparing arbitrary single-photon tripartite entangled states. We present evidence for the proper operation of this protocol by measuring the time-dependent behavior of the two phase qubits. Here, entanglement is not verified

2

directly, but the data are consistent with theoretical predictions. Proper execution of this protocol can prepare the system in a Bell or W-state, as well as arbitrary entangled states.

In Fig. 1a, we show an optical micrograph of two qubits, qubit 1 and qubit 2, capacitively coupled to either end of an open-ended coplanar waveguide cavity whose half-wave resonant mode frequency is $\omega_c/2\pi \approx 8.9$ GHz. These cavities have shown coherent properties at the single-photon level.[14] Flux-biased phase qubits[25] can be thought of as anharmonic LC-oscillators in which a single Josephson junction provides enough nonlinearity to address the two lowest oscillatory phase states $|g\rangle$ and $|e\rangle$. The energy level separation $\hbar\omega_j \equiv E_e - E_g$ can be independently tuned over a range $\sim 7\,\text{GHz}-10\,\text{GHz}$ on the j-th qubit by use of inductively coupled flux bias coils. An additional coil allows us to apply microwave pulses and fast bias shifts, also used for single-shot state measurement.[14] Independent state readout on the j-th qubit is accomplished by use of an inductively coupled dc superconducting quantum interference device (SQUID). We describe this system using a two-qubit Jaynes-Cummings or Tavis-Cummings model.[26] In a frame rotating at an reference frequency ω_μ, we approximate the Hamiltonian of the system as

$$H = \hbar\Delta_c a^\dagger a + \sum_{j=1,2} \left[\hbar\Delta_j \sigma_j^+ \sigma_j^- + i\hbar g_j(\sigma_j^+ a - a^\dagger \sigma_j^-) \right], \tag{1}$$

where the mode operators $\sigma_j^\pm$ and $a^{(\dagger)}$ refer to the qubits and the cavity, respectively, with corresponding detunings $\Delta_j/\hbar \equiv \omega_j - \omega_\mu$ and $\Delta_c/\hbar \equiv \omega_c - \omega_\mu$. Capacitive coupling C_c between the qubits and the cavity results in an effective coupling frequency of $2g_j/2\pi \approx \omega_c/2\pi\ C_c/\sqrt{CC_J} \approx 2g/2\pi \sim 90$ MHz for both qubits. The system exhibits decay rates of $\gamma_1/2\pi \sim 7$ MHz, $\gamma_2/2\pi \sim 10$ MHz, and $\kappa/2\pi \sim 1$ MHz for each qubit and the cavity, respectively. We denote the product of two qubit-cavity states as $|\eta\eta' n\rangle \equiv |\eta\rangle_1 \otimes |\eta'\rangle_2 \otimes |n\rangle_c$, where $|\eta\rangle_j$ label the j-th qubit state ($|g\rangle$ or $|e\rangle$) and n

labels the cavity Fock state.

The first signature of tripartite interactions is revealed by spectroscopic measurements[23,24] as a function of the detuning $\Delta_{1,c}/\hbar = \omega_1 - \omega_c$ of qubit 1 when qubit 2 and the cavity are resonant ($\omega_2 = \omega_c$). In the case of a single qubit-cavity system, the Jaynes-Cummings model predicts a single vacuum Rabi-mode splitting of the qubit state.[14] Here, the single qubit states are split twice by the mutual interaction of all three systems, as shown in Fig. 1b. We can interpret this as due to the coupling between the bare qubit 1 and the antisymmetric pair of maximally entangled Bell states between qubit 2 and the cavity. The two avoided crossings in the spectrum occur along the qubit 1 detuning curve, symmetrically displaced about the tripartite resonance ($\omega_1 = \omega_2 = \omega_c$). These measured curves agree well with a full analysis of the two-qubit Jaynes-Cummings or Tavis-Cummings[24] model.

With independent control over both qubits, we can easily explore a convenient state-space whereby a single photon of energy $\hbar\omega_c$ is shared by our tripartite system. Using a similar technique established for inducing coherent interactions between a single qubit and a cavity[14], we investigate the evolution of vacuum Rabi oscillations between qubit 1 and the cavity as a function of the detuning of qubit 2 $\Delta_{2,c}/\hbar = \omega_2 - \omega_c$ from the joint qubit 1-cavity system ($\omega_1 = \omega_c$). For simplicity, we use the term "photon" even when describing a single excitation in the qubit. We begin with both qubits in their ground state and qubit 1 far off-resonance from the cavity (see pulse diagram in Fig.2a), then we excite qubit 1 with a photon using a π pulse and bring it onto resonance with the cavity (using a shift pulse) for a given evolution time period t_e followed by simultaneous measurement of both qubits[12]. When qubit 2 is far enough off-resonant, the resultant vacuum Rabi oscillations are

characterized by the frequency $\Omega_0 \equiv 2\,g$, as seen on either side of Fig. 2b,d. Here, the exchange between qubit 2 and the qubit 1-cavity system is energetically prohibited, so that qubit 1 undergoes basic vacuum Rabi oscillations with the cavity alone. However, when all three systems are on-resonance with each other, the photon begins in qubit 1 and then 'spreads out' to the cavity until becoming shared also with qubit 2, eventually moving completely to qubit 2. As time progresses, the photon eventually returns to qubit 1.

In this anti-symmetric mode, the oscillation frequency is given by $\Omega_a = \Omega_0/\sqrt{2}$. As the system evolves, the photon is never completely transferred to the cavity. There are times when the photon is entirely in qubit 1 or entirely in qubit 2, otherwise the system occupies a continuum of entangled states of both qubits and the cavity (see Fig. 2f). By measuring the two qubit simultaneously[12], we can extract the joint probabilities P_{eg0} and P_{ge0} for single-photon states $|eg0\rangle$ and $|ge0\rangle$, respectively. A theoretical model including the finite rise-time of the shift pulse (~ 10 ns) agrees well with the experimental data (Fig. 2d-f).

The above experiment lends itself to a simple geometric description that can help us visualize the system dynamics. By use of equation (1), we can identify the unitary evolution $U(t) = e^{-iHt/\hbar}$ of the system with a three-dimensional rotation $R_{\mathbf{n}}(\varphi) = e^{-i\mathbf{n}\cdot\mathbf{X}\varphi}$ about $\mathbf{n} \equiv (0, g_2, -g_1)/\sqrt{g_1^2 + g_2^2}$ with $\varphi = \sqrt{g_1^2 + g_2^2}\,t$ and $\mathbf{X} \equiv (X_1, X_2, X_3)$. Here, $(X_k)_{ij} = -i\epsilon_{ijk}$ helps generate the rotation, and ϵ_{ijk} is the totally antisymmetric Levi-Civita tensor. Time evolution of the system then corresponds to orbits on a unit sphere azimuthal to the vector $\mathbf{n}$, where $(x, y, z) \Leftrightarrow (|gg1\rangle, |eg0\rangle, |ge0\rangle)$, as shown in Fig. 2g,h. By taking the amplitudes of the three coupled states as real, absorbing any overall phase into a redefinition of the states, we can construct a (unit) state vector analogous to

that used for a single spin-1/2 system on the Bloch sphere. In this case, as the state vector precesses about $\mathbf{n}$ and away from any of the coordinate axes, entanglement evolves over time between all three systems. For the experiment described above, we start with an initial condition corresponding to the state $|eg0\rangle$. When qubit 2 is far off-resonance (Fig. 2g), the system precesses at Ω_o about $\mathbf{n} = (0, 0, 1)$, showing simple vacuum Rabi oscillations between qubit 1 and the cavity involving the states $|eg0\rangle$ and $|gg1\rangle$, generating bipartite entanglement. However, when all three systems are on-resonance ($\omega_1 = \omega_2 = \omega_c$), $H = g_2 X_2 - g_1 X_3 = g(X_2 - X_3)$, $\mathbf{n} = (0, 1, -1)/\sqrt{2}$, and $\varphi = \sqrt{2} g\, t$ leading to a "tripartite evolution". Now the initial state vector $|eg0\rangle$ precesses about $\mathbf{n}$ so that the trajectory passes from the $|eg0\rangle$-axis into a region where the photon is shared with the cavity and then through the $-|ge0\rangle$-axis (see Fig. 2h). The oscillations in the two qubits then follow the anti-symmetric mode frequency Ω_{a}. This single-photon "tripartite sphere" representation provides an intuitive picture for visualizing the equivalence between entangled states in the same class.[19] In this case, the local operations are vacuum Rabi oscillations or tripartite evolution. We can see that any arbitrary single-photon tripartite state can be created and subsequently transformed into any other state on the tripartite sphere, much like unitary operations and rotations on the Bloch sphere. Of particular interest is the fact that a specific initial state will follow a specific trajectory under tripartite evolution, transforming the amount of entanglement continuously. Below, we determine the conditions for directly demonstrating transformations between Bell and W states, starting from an initially pure state.

We begin with a single photon in qubit 1 or qubit 2. As shown above, vacuum Rabi oscillations represent arbitrary rotations in the $|gg1\rangle$-$|eg0\rangle$ plane (between the cavity and qubit 1) or the $|gg1\rangle$-$|ge0\rangle$ plane (cavity and qubit 2). These two operations in succession allow us complete access

to the $|eg0\rangle$-$|ge0\rangle$ plane, and, thus, the ability to prepare any initial state on the entire single-photon tripartite sphere. In order to generate Bell and W states, we can start with the photon in the cavity, $|gg1\rangle$. Under tripartite evolution the system passes first through the W state, $|\text{W}\rangle \equiv (-|gg1\rangle + |eg0\rangle + |ge0\rangle)/\sqrt{3}$, and then through the Bell state, $|\text{Bell}\rangle \equiv -(|eg0\rangle + |ge0\rangle)/\sqrt{2}$, as the system vector rotates about the n-vector, $\mathbf{n} = (0, 1, -1)/\sqrt{2}$ as shown in Fig. 3b. In total, the system will pass through two Bell states and four W states for one full revolution about $\mathbf{n}$. The frequency $\Omega_{\text{s}} = \sqrt{2}\,\Omega_0$ of qubit oscillations follows from the definition of φ and the arc traced out by the system trajectory. In this symmetric mode ($\Omega_{\text{s}} = 2\Omega_{\text{a}}$) the photon "splits" as it leaves the cavity, having an equal probability for going to qubit 1 or qubit 2, and subsequently returning completely to the cavity.

Experimentally, we sample a variety of initial states by allowing qubit 1 (which initially has the photon) to undergo vacuum Rabi oscillations with the cavity for a delay time period t_{d} before we bring qubit 2 into tripartite resonance. Fig. 3c-e shows a prediction for the unitary evolution of the system for nearly a continuum of values for t_{d}. Here, the joint probabilities are P_{gg1}, P_{eg0}, and P_{ge0} for states $|gg1\rangle$, $|eg0\rangle$, and $|ge0\rangle$, respectively. Notice that for $t_{\text{d}} = 2\pi/\Omega_0$, the system will exhibit the anti-symmetric mode (indicated along the dashed line) as described earlier. However when $t_{\text{d}} = \pi/\Omega_0$, we prepare the (initial condition) $|gg1\rangle$, allowing for a tripartite evolution of the symmetric mode. After a period of time $t_e = \pi/4\Omega_{\text{s}}$, the excited-state probability for both qubits is 1/3 and the system is in the $|\text{W}\rangle$-state, with the photon equally distributed among the two qubits and cavity. After a period of time $t_e = \pi/2\Omega_{\text{s}}$, the excited-state probability for both qubits is 1/2 and the system is in the bipartite $|\text{Bell}\rangle$-state. These points are indicated in Fig. 3c-e, with the first three states shown as vectors on the tripartite sphere in Fig. 3b. Here the simulations have included

finite energy relaxation and the rise-time of the shift pulses.

We simultaneously measure both qubits and observe the occupation probabilities of the two qubits over time as they evolve from a continuum of initial states, superposition states of qubit 1 and the cavity. Although possible, as explained later, we do not measure the cavity state directly. Fig. 4c,d shows extracted line cuts from Fig. 4a,b for two initial conditions (dashed lines) corresponding to the symmetric and anti-symmetric modes. As can been seen from Fig. 3d,e, the theoretical predictions for the evolutions agree with the measurements. For the symmetric mode we find in-phase oscillations of the two qubits at $\Omega_{\text{s}} \sim \sqrt{2}\,\Omega_0$, while for the anti-symmetric mode, we find that the two qubits oscillate out of phase with each other with the anti-symmetric mode frequency $\Omega_{\text{a}} \sim \Omega_0/\sqrt{2}$, where Ω_0 is the frequency of the vacuum Rabi oscillations that occur during the delay time period t_{d} (lower right hand corner of Fig. 4a). The measured frequencies agree within $\sim 15\,\%$ of the ideal case, due to the finite rise-time of the shift pulses and some residual nonzero detuning of each qubit frequency. A theoretical model including these imperfections (solid lines) agrees well with the data.

In the present experiment, we improved the previous design[14,27] by reducing the qubit junction areas to reduce the number of two-level system defects. This more than doubled the qubit visibility and provided the necessary 'clean' cavity region for observing tripartite interactions. However, it was not possible to perform two-qubit state tomography over the required time scales due to short relaxation times[28] matched with the continued presence of two-level system defects that limited the qubit visibility[29] to $\lesssim 50\,\%$. With further reductions in junction size, we can raise the single qubit visibility to 90% allowing full tomographic characterization of both qubits.[13]

In the future, we intend to perform correlated measurements and tomography of this tripartite system. This requires a fast, dispersive measurement and readout of the qubits to solve three difficulties. First, the tunneling-based measurement of either qubit will populate the cavity with unwanted photons due to a crosstalk process.[12] Second, a dispersive measurement will increase qubit visibility ensuring clear tomography. And third, after measurement of the two qubits, subsequent qubit rotations will ensure proper state preparation for one of the qubits, making it ready for re-interaction with the cavity. In this way, we can reuse one of the qubits through state transfer[14], to fully determine the cavity state[30]. Improvements are currently underway to modify our slow switching-current SQUID readout to a fast, dispersive resonant readout.

Tripartite interactions provide a means of engineering qubit entangled states. We have provided a theoretical description of the two-qubit Jaynes-Cummings or Tavis-Cummings model and a free-evolution protocol for the deterministic preparation of Bell, W, or arbitrary entangled states with one shared photon. This includes a convenient geometric description helpful for visualizing the unitary evolution. We have presented clear experimental evidence of tripartite interactions between two

1. Gottesman, D. & Chuang, I. L. Demonstrating the viability of universal quantum computation using teleportation and single-qubit operations. *Nature* **402**, 390 (1999).

2. Karlsson, A. & Bourennane, M. Quantum teleportation using three-particle entanglement. *Phys. Rev. A* **58**, 4394 (1998).

3. Briegel, H. J., Dür, W., Cirac, J. & Zoller, P. Quantum repeaters: The role of imperfect local

operations in quantum communication. *Phys. Rev. Lett.* **81**, 5932 (1998).

4. Hillery, M., Buzek, V. & Berthiaume, A. Quantum secret sharing. *Phys. Rev. A* **59**, 1829 (1999).

5. Greenberger, D. M., Horne, M. A. & Zeilinger, A. Multiparticle interferometry and the superposition principle. *Physics Today* **46**, 22–29 (1993).

6. Giovannetti, V., Lloyd, S. & Maccone, L. Quantum-enhanced measurements: Beating the standard quantum limit. *Science* **306**, 1330 (2004).

7. Leibfried, D. *et al.* Creation of a six-atom Schrödinger cat state. *Nature* **438**, 639–641 (2005).

8. Roos, C. F. *et al.* Control and measurement of three-qubit entangled states. *Science* **304**, 1478–1482 (2004).

9. Pan, J.-W., Bouwmeester, D., Daniell, M., Weinfurter, H. & Zeilinger, A. Experimental test of quantum nonlocality in three-photon Greenberger-Horne-Zeilinger entanglement. *Nature* **403**, 515–519 (2000).

10. Rauschenbeutel, A. *et al.* Step-by-step engineered multiparticle entanglement. *Science* **288**, 2024–2028 (2000).

11. Yamamoto, T., Yu. A. Pashkin, Astafiev, O., Nakamura, Y. & Tsai, J. S. Quantum oscillations in two coupled charge qubits. *Nature* **425**, 941 (2003).

12. McDermott, R. *et al.* Simultaneous state measurement of coupled Josephson phase qubits. *Science* **307**, 1299–1302 (2005).

13. Steffen, M. *et al.* Measurement of the entanglement of two superconducting qubits via state tomography. *Science* **313**, 1423–1425 (2006).

14. Sillanpää, M. A., Park, J. I. & Simmonds, R. W. Coherent quantum state storage and transfer between two phase qubits via a resonant cavity. *Nature* **449**, 438–442 (2007).

15. DiCarlo, L. *et al.* Demonstration of two-qubit algorithms with a superconducting quantum processor. *Nature* **460**, 240–244 (2009).

16. Niskanen, A. O. *et al.* Quantum coherent tunable coupling of superconducting qubits. *Science* **316**, 723–726 (2007).

17. Hao, C.-F., J.-C. Li & Guo, G.-C. Controlled dense coding using the Greenberger-Horne-Zeilinger state. *Phys. Rev A* **63**, 054301 (2001).

18. Borsten, L., Dahanayake, D., Duff, M. J., Ebrahim, H. & Rubens, W. Wrapped branes as qubits. *Phys. Rev. Lett.* **100**, 251602 (2008).

19. Dür, W., Vidal, G. & Cirac, J. Three qubits can be entangled in two inequivalent ways. *Phys. Rev. A* **62**, 062314 (2000).

20. Wei, L. F., Liu, Y.-x. & Nori, F. Greenberger-Horne-Zeilinger entanglement in superconducting circuits. *Phys. Rev. Lett.* **96**, 246803 (2006).

21. Galiautdinov, A. & Martinis, J. M. Maximally entangling tripartite protocols for Josephson phase qubits. *Phys. Rev. A* **78**, 010305 (2008).

22. Kim, M. D. & Cho, S. Y. Macroscopic Greenberger-Horne-Zeilinger and W states in flux qubits. *Phys. Rev. B* **77**, 100508 (2008).

23. Xu, H. *et al.* Spectroscopy of three-particle entanglement in a macroscopic superconducting circuit. *Phys. Rev. Lett.* **94**, 027003 (2005).

24. Fink, J. M. *et al.* Dressed collective qubit states and the tavis-cummings model in circuit qed. *Phys. Rev. Lett.* **103**, 083601 (2009).

25. Simmonds, R. W. *et al.* Decoherence in Josephson phase qubits from junction resonators. *Phys. Rev. Lett.* **93**, 077003 (2004).

26. Tavis, M. & Cummings, F. W. Exact solution for an n-molecule-radiation-field hamiltonian. *Phys. Rev.* **170**, 379–384 (1968).

27. Simmonds, R. W. *et al.* Coherent interactions between phase qubits, cavities, and tls defects. *Quantum Information Processing* **8**, 117–131 (2009).

28. Martinis, J. M. *et al.* Decoherence in Josephson qubits from dielectric loss. *Phys. Rev. Lett.* **95**, 210503 (2005).

29. Cooper, K. B. *et al.* Observation of quantum oscillations between a Josephson phase qubit and a microscopic resonator using fast readout. *Phys. Rev. Lett.* **93**, 180401 (2004).

30. Hofheinz, M. *et al.* Synthesizing arbitrary quantum states in a superconducting resonator. *Nature* **459**, 546–549 (2009).

superconducting phase qubits and a resonant microwave cavity. Our system has a fundamental advantage over strictly multi-qubit systems[20–22]: The cavity provides a larger degree of freedom as opposed to the two discrete levels associated with qubits and can be thought of as a multiphoton

register or entanglement resource. Arbitrary preparation of multiphoton states in this cavity via one of the qubits[30], and subsequent interactions for entanglement distribution will allow for the creation of further classes of entanglement, such as a GHZ state.

Author Information   Reprints and permissions information is available at www.nature.com/reprints. The authors declare no competing financial interests. Correspondence and requests for materials should be addressed to R.W.S. (simmonds@boulder.nist.gov).
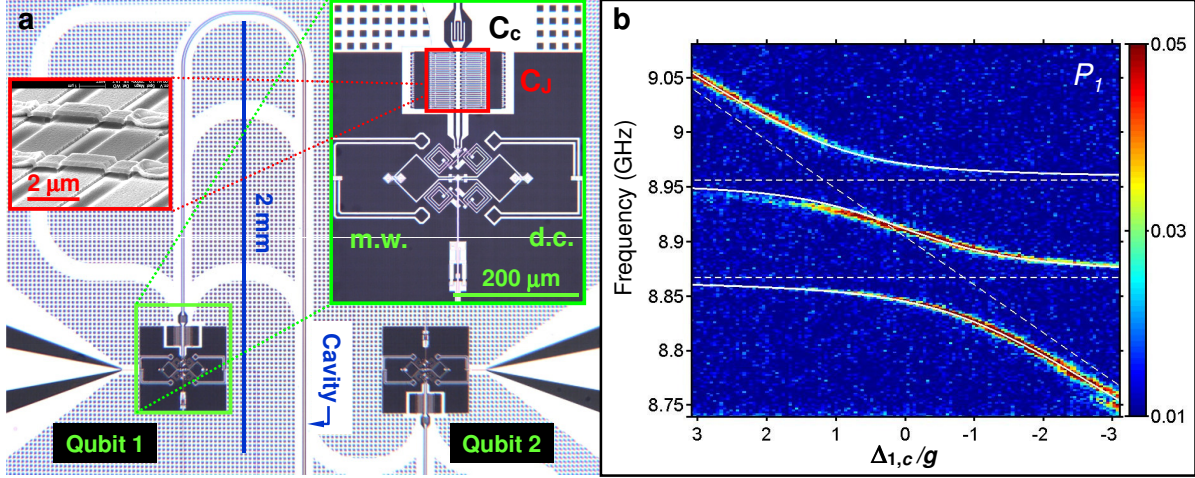
Figure 1: Circuit and spectroscopy. **a**, Optical micrograph of the electrical circuit with two Josephson phase qubits (qubit 1 inset overlay right), each with loop inductance $\sim$700 pH and critical current ~ 0.91 μA (junction areas ~ 6 μm^2) shunted by use of interdigitated capacitors ($C_J \sim 0.7$ pF, including junction capacitance) with vacuum gap crossovers (inset overlay left), capacitively coupled ($C_c \sim 6.2$ fF) to a coplanar waveguide resonant cavity (of full length ~ 7 mm). The device was fabricated with standard optical lithography with Al/AlO$_x$/Al junctions on a sapphire substrate, with SiO$_2$ as an insulator surrounding the junctions. **b**, Microwave spectroscopy of qubit 1 as a function of detuning $\Delta_{1,c} = \omega_1 - \omega_c$ with $\omega_2 = \omega_c$. $\Delta_{1,c}$ is varied through the d.c. flux bias coils and qubit 1 is excited by microwaves applied through the m.w. (microwave) coil (seen in **a**). The intensity color scale represents the probability of qubit 1 tunneling after the measure pulse. The dashed diagonal line shows the bare qubit 1 transition frequency. The dashed horizontal lines represent the two maximally entangled Bell states between qubit 2 and the cavity.
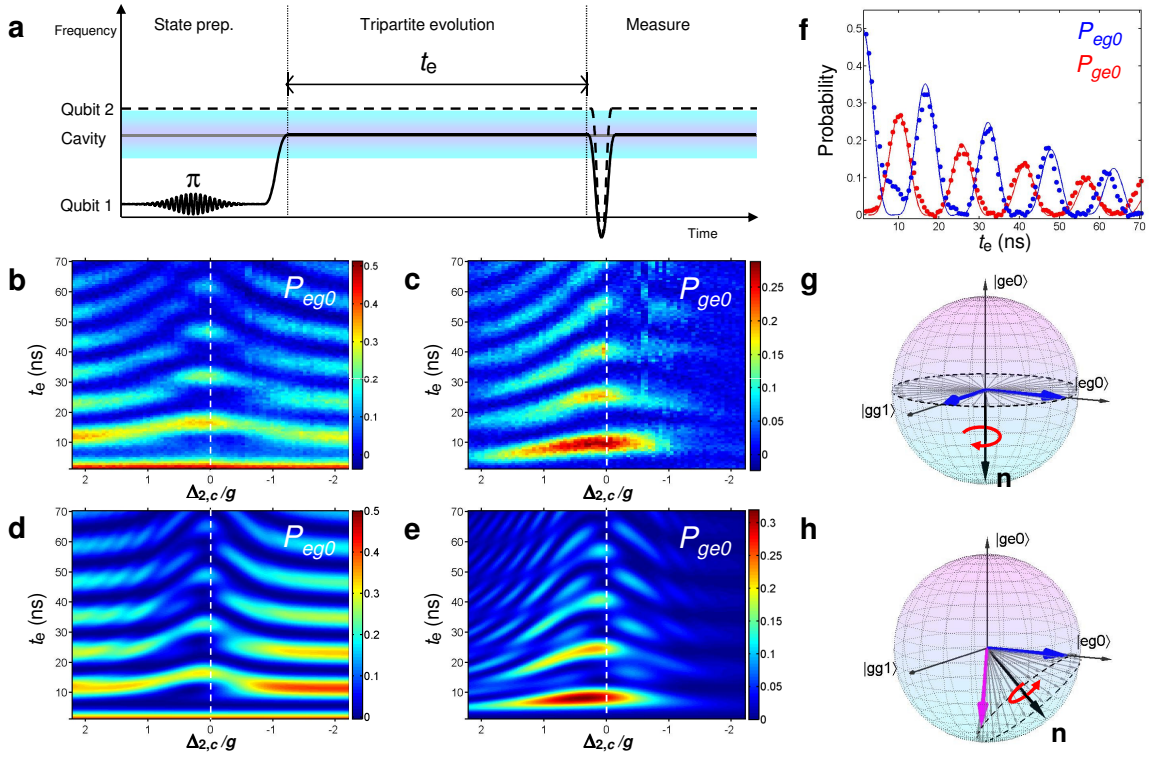
Figure 2: Demonstration of basic tripartite interactions. **a**, Description for creating a photon in qubit 1 by use of a π pulse, then shifting (solid line) onto resonance with the cavity and qubit 2 for various qubit 2 detunings (dashed line). After an evolution time period t_e the qubits are measured simultaneously[12]. **b,c**, Measured excited state joint probabilities P_{eg0} and P_{ge0} for states $|eg0\rangle$ and $|ge0\rangle$, respectively, during tripartite interactions after qubit 1 has been excited by a π pulse and shifted onto resonance with the cavity as a function of the detuning $\Delta_{2,c} = \omega_2 - \omega_c$ of qubit 2. **d,e**, Theoretical predictions including qubit visibility and finite rise-time of the shift pulse. The resulting asymmetry is relatively insensitive to the exact shape of the shift pulse and can be attributed to additional interference due to finite detuning of $\sim 0.3g$. Here, we used an exponential rise-time of ~ 10 ns. **f**, Line cut of the on resonance tripartite interactions with corresponding theoretical prediction (solid line). **g,h**, The red arrow provides a visual cue to the circular trajectory of the tripartite vector. **g**, Tripartite sphere representation during simple vacuum Rabi oscillations of qubit 1. **h**, Tripartite sphere representation during the tripartite evolution from the initial state $|eg0\rangle$.
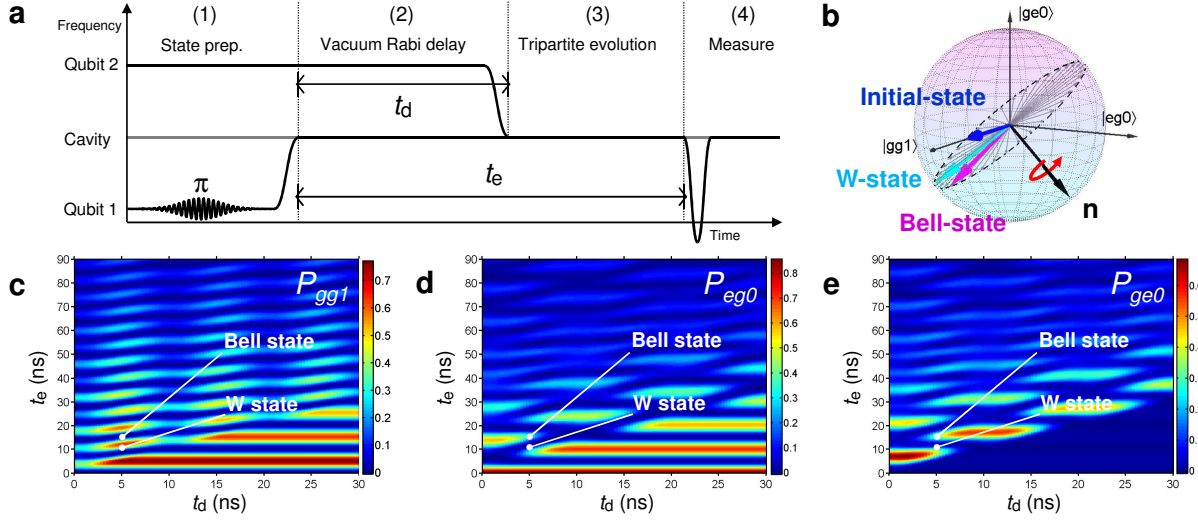
15

Figure 3: Experimental protocol and theoretical predictions for generating generalized arbitrary single photon tripartite evolutions. **a**, Pulse sequence: (1) A photon is inserted in the system by exciting qubit 1. (2) A shift pulse brings qubit 1 onto resonance with the cavity, producing vacuum Rabi oscillations. (3) A shift pulse brings qubit 2 onto resonance after the delay time t_{d}, initiating tripartite interactions that evolve over a time period $t_{\mathrm{e}} - t_{\mathrm{d}}$. (4) Both qubits are measured simultaneously. **b**, Tripartite sphere representation of the tripartite evolution for the initial state $|gg1\rangle$ prepared during a delay time period $t_{\mathrm{d}} = \pi/\Omega_o$. The red arrow provides a visual cue to the circular trajectory of the tripartite vector. **c**, Predicted state occupation of one photon in the resonant cavity. **d,e**, Predicted joint state probabilities P_{eg0} and P_{ge0} for measurement of qubit 1 and 2 as functions of both t_{d} and t_{e}. Blue color represents low values, red represents high. The simulations were performed with a finite energy relaxation time, a finite shift pulse rise-time (~ 10 ns), and some residual qubit detuning of $\sim 0.3g$ from the cavity.
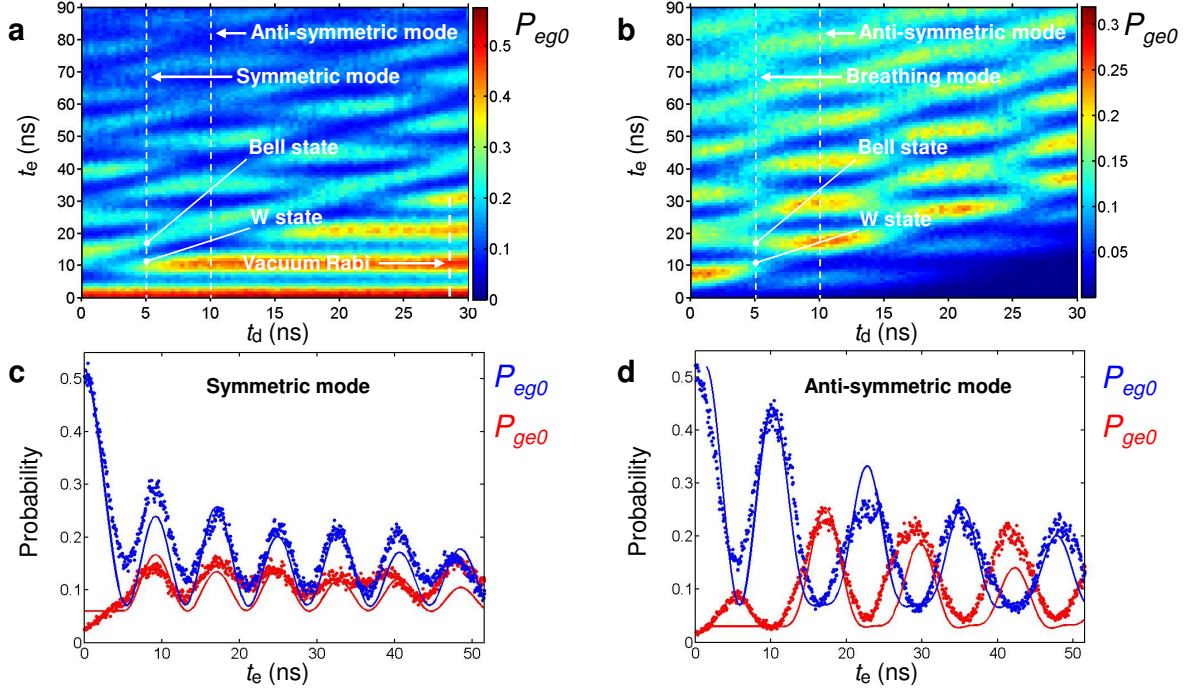
Figure 4: Experimental demonstration of arbitrary tripartite interactions between both phase qubits and the cavity. **a,b**, Measured joint state probabilities P_{eg0} and P_{ge0} for measurement of qubit 1 and 2 as functions of both t_d and t_e. **c**, Extracted curves (along dashed line) for the initial state $|gg1\rangle$ producing a tripartite evolution of the symmetric mode, showing in phase oscillations along with theoretical predictions (solid lines) from Fig. 3d,e. During this evolution, the system's entanglement continuously transforms starting from a pure state $|gg1\rangle$. In the ideal case, the system evolves through W and Bell states. **d**, Extracted curves (along dashed line) for the initial state $|eg0\rangle$ producing a tripartite evolution of the anti-symmetric mode, showing out of phase oscillations along with theoretical predictions (solid lines) from Fig. 3d,e.